Macroporous Ceramics from Ceramic-Polymer Dispersion Methods

Nancy Wara Androff and Lorraine F. Francis
Dept. of Chemical Engineering and Materials Science, University of Minnesota, Minneapolis, MN 55414

Bhaskar V. Velamakanni
3M Company, St. Paul, MN 55144

Porous ceramics were fabricated by firing ceramic-polymer composites prepared by casting dispersions containing cellulose acetate, water and colloidal ceramic particles (alumina and silica). Composite microstructures were determined by polymer phase separation. Polymer adsorption on the ceramic particles was necessary for the formation of controlled porosity in the composite and fired ceramic. Cellulose acetate adsorbed on alumina, but not silica particles. The microstructure of alumina-cellulose acetate composites was characterized by unagglomerated alumina particles in a polymer matrix; relatively large pores (pore diameter ~ 15μm) formed when the alumina concentration was low (< 50 vol. % relative to the polymer in the dried composite), and smaller pores (pore diameter ~ 2μm) developed at higher alumina contents. By contrast, silica-cellulose acetate composites contained agglomerated silica particles and a large pore structure invariant to silica content. Firing of alumina-cellulose acetate composites with ceramic contents greater than 40 vol. % resulted in crack-free porous ceramics with pore structures comparable to the original composites.

Introduction

Porous ceramics are gaining importance in a variety of applications, including filters and membranes, electronics, and biomaterials (Sheppard, 1993; Schaefer, 1994; Marquis, 1993). Ceramics have advantages compared with similarly porous polymeric materials in these applications due to their thermal properties, corrosion resistance, electrical and acoustic properties, and wear behavior (Sheppard, 1993; Schaefer, 1994). Currently, ceramics with pore sizes from the angstrom to the millimeter range can be prepared by employing a variety of methods ranging from sol-gel to micelle templeting to physical machining (Sheppard, 1993; Davis, 1993; Brave, 1991; Smith, 1989). The current methods used to manufacture porous ceramics, however, have a number of limitations. For example, physical machining and chemical leaching have involved processing steps and can only achieve a narrow range of pore structures (Sheppard, 1993; Schaefer, 1994). Sol-gel is a simpler process, but it cannot currently achieve orientation of pores in a specific direction (de Lange et al., 1995; Kim, 1995; Klein and Giszpenc, 1990). Micelle templating methods offer more flexibility in processing and pore structure tailoring. However, these techniques typically lead to a granular dried product rather than to a coherent piece of ceramic, and the final ceramics are not always completely crystalline (Tanev and Pinnavaia, 1996; Davis, 1993). Consequently, although porous ceramics have highly desirable properties, difficulties remain in processing.

Porous polymers, on the other hand, can be prepared in a wide variety of microstructures using phase separation. For example, "phase inversion" membranes are porous polymer sheets used in separation applications such as reverse osmosis and ultrafiltration. These membranes are made from a variety of polymers including cellulose derivatives, polyimides, polyamides, and polysulfones (Kesting and Fritzsche, 1993; McDonogh et al., 1987). The term phase inversion refers to the phase separation process in which the discontinuous polymer phase becomes continuous (Kesting and Fritzsche, 1993). In one version of this process, a polymer and solvent (and optionally a nonsolvent) are cast onto a substrate and immersed in a nonsolvent bath. The immersion leads to the phase separation of the polymer, and, ultimately, results in

Correspondence concerning this article should be addressed to L. F. Francis.

an asymmetric membrane with a thin (~ 1 μm) dense layer at the coating/nonsolvent bath interface and a thick (~ 100 μm) porous underlayer (Smolders et al., 1992; Tsay and McHugh, 1990). The pore structure of the underlayer can be varied from uniformly spaced pores (10–50 μm diameter), which are oriented through the coating thickness (these pores are referred to as macrovoids) to a more uniform smaller pore network (1–2 μm diameter) (Smolders et al., 1992; Mulder et al., 1985).

The ability to create a variety of controlled and complex pore structures in polymer phase inversion systems suggests a new processing route for porous ceramics. If a ceramic phase could be incorporated into these systems without adversely affecting the polymer microstructure, then a porous ceramic could be achieved by making a composite membrane and burning out the polymer. We previously reported that a ceramic phase can be successfully added to a polymer phase inversion system (Wara et al., 1995). Alumina particles were added to the most studied of these systems: cellulose acetate/acetone/water. Free standing composites containing alumina particles well distributed within a continuous polymer matrix were prepared. By varying the ceramic content in the initial casting dispersion, the structure of the composites could be shifted (as it can by other means in polymer systems) from large pores (15 μm) to a smaller pore network (1–2 μm).

This article discusses the ability to make controlled porosity composites and to fire these composites to give macroporous ceramics. The first part concerns the control of the composite microstructure by varying the ceramic content and ceramic-polymer interactions in the dispersion. The second focuses on firing the composite to prepare a porous ceramic. The microstructures of the composite and porous ceramic will be compared, and particle-particle consolidation and shrinkage discussed.

Experimental Procedure

Composite preparation and characterization

Composites were prepared from dispersions containing ceramic particles and cellulose acetate polymer. The ceramic (alumina or silica particles) was first dispersed in water. The alumina particles (Alcoa SG16) had an average particle diameter of 0.34 μm and were electrostatically stabilized with hydrochloric acid in deionized water at pH 4. The silica particles (Ludox AS40) had an average particle size of 22 nm. The silica was electrostatically stabilized in water by the manufacturer using ammonium hydroxide (pH ~ 9). The cellulose acetate (Aldrich, mol. wt ~ 30,000 g/mol) was dissolved in acetone. The polymer solution and the ceramic dispersion were mixed (sometimes with added water and acetone) to give dispersions with a fixed acetone:water:cellulose acetate volume ratio of 23:6.5:1 and varying amounts of ceramic. While water is a nonsolvent for cellulose acetate, the dispersion composition was chosen in the single-phase region of the ternary cellulose acetate-acetone-water phase diagram (Strathmann et al., 1971; Shojaie et al., 1994). The combined dispersions were coated onto glass plates (6.4 cm $\times$ 6.4 cm) using manual draw down of a doctor blade with a fixed gap width of 0.5 mm. The coatings were immersed in a water bath for 5 min (after immersion, the coatings detach from the substrates to give free standing films) and dried for 24 h at ambient conditions. Further details on dispersion preparation and coating methods are given elsewhere (Wara et al., 1995). The dried coatings had relative volume percentages of ceramic (total ceramic in the dried film compared to the total solids content of the dried film) ranging from approximately 10 to 60%.

The microstructures of the dried composites were examined using scanning electron microscopy (SEM). Plan view and cross-sectional images were obtained using a JOEL 840. Secondary and backscattered images were acquired with a Hitachi 900 field emission gun scanning electron microscope (FEG SEM).

Dispersion characterization

Adsorption isotherms were constructed for alumina and silica in the presence of cellulose acetate using thermogravimetric analysis (TGA). For this experiment, dispersions were prepared with a fixed ceramic content and a variable cellulose acetate content. One gram of ceramic was dispersed in 15 mL of a 3.6:1 by volume acetone:water solution (the experimental ratio of acetone to water in the coated dispersions). Hydrochloric acid was added to adjust the pH to 4. The pH of the silica was set at 9 by the manufacturer. Varying amounts of cellulose acetate (0.01 to 4 g) were added to the stabilized ceramic dispersions. The samples were allowed to equilibrate for 24 h. The samples were then washed five times with acetone to remove free cellulose acetate and dried in ambient conditions for 48 h. The amount of adsorbed polymer was measured with TGA using a Perkin-Elmer TGA 7. Samples were ramped at 10°C/min from 30 to 800°C under an air atmosphere. Based on TGA of pure cellulose acetate under the same conditions, weight loss in the range from 200–600°C was attributed to adsorbed cellulose acetate. The value obtained from TGA was converted to mg adsorbed cellulose acetate per m^2 ceramic particle surface area.

Sedimentation was used to examine the stability mechanisms of alumina and silica at the experimental solvent conditions and in the presence of cellulose acetate. First, 2.5 vol. % dispersions of alumina and silica were made with increasing acetone:water ratios (without cellulose acetate). Alumina and silica were electrostatically stabilized as described above. Second, similar dispersions were made at the experimental acetone:water ratio (3.6:1), and the cellulose acetate concentration was varied from 0 to 63 vol. % relative to the ceramic. All the dispersions were placed in 100 mL graduated cylinders and allowed to stand for 72 h. The sediment height in each cylinder was then measured. Sediment height was normalized to give a relative stability based on the most stable dispersion for each ceramic.

Composite firing and polymer burnout characterization

Composites of alumina and cellulose acetate were fired in air in a Lindberg high-temperature box furnace. The specimens were heated at 1°C/min to 1,100°C and then held at 1,100°C for 3 h. They were then heated with a rapid ramp rate (50°C/min) to 1,400°C and held there for 0.5 h to partially sinter the alumina particles. The microstructures of the fired alumina films were observed using SEM (JEOL 840).

The behavior of cellulose acetate before decomposition was observed using dynamic mechanical analysis (DMA, Perkin-

Elmer System 7e). A cellulose acetate film was made by casting a 20 wt. % cellulose acetate in acetone solution onto a glass slide and allowing the acetone to evaporate. The dense cellulose acetate film was removed from the substrate by soaking in water and then dried at room temperature. Polymer glass transition behavior was observed using the DMA flat punch (1-mm disk) configuration with a static force of 50 mN. A 5°C/min ramp rate was used from 10–200°C, and the sample was run in an air atmosphere.

Polymer burnout from the alumina-cellulose acetate composites was tracked with TGA and differential thermal analysis (DTA, Perkin-Elmer System 7/4 Thermal Analysis Controller). For both methods, a 10°C/minute ramp rate was used from 50–700°C, and all samples were run in an air atmosphere. Films with relative alumina contents of up to ~60 vol. % were tested.

Microstructure studies of polymer burnout from alumina-cellulose acetate composites were performed using FEG SEM and TGA. A composite with a relative alumina content of 42 vol. % was sectioned into 1 cm×1 cm pieces. The polymer burnout region for the composite was tracked using TGA. A 1°C/min ramp rate from 50–700°C under air was used to match the composite firing conditions. Based on the TGA results, the 1 cm×1 cm pieces were separately heated to selected temperatures in the polymer burnout region. The samples were air-quenched upon reaching temperature. The microstructures of the samples were examined using secondary and backscattered FEG SEM at an acceleration voltage of 10 kV.

Shrinkage during polymer burnout in alumina-cellulose acetate composites was measured and also investigated by mercury porosimetry. The width, length, and thickness of pre- and post-fired composites were measured using a digital micrometer and a Mitutoyo thickness gage (#543-110). For composites with 40, 50 and 60 relative vol. % alumina, the percentage of shrinkage based on volume was calculated by averaging measurements from eight samples per alumina content. Mercury porosimetry was performed using a Micrometerics 9230 Pore Sizer. Plots of incremental mercury intrusion volume as a function of pore size were generated for pre- and post-fired composites.

Results

Composite microstructure

The effect of increasing the alumina content of the microstructure of alumina-cellulose acetate composites is shown in Figure 1. SEM micrographs of the surface which was in contact with the substrate (referred to as the bottom surface) are shown for the 20, 42, 54 and 62 relative vol. % alumina

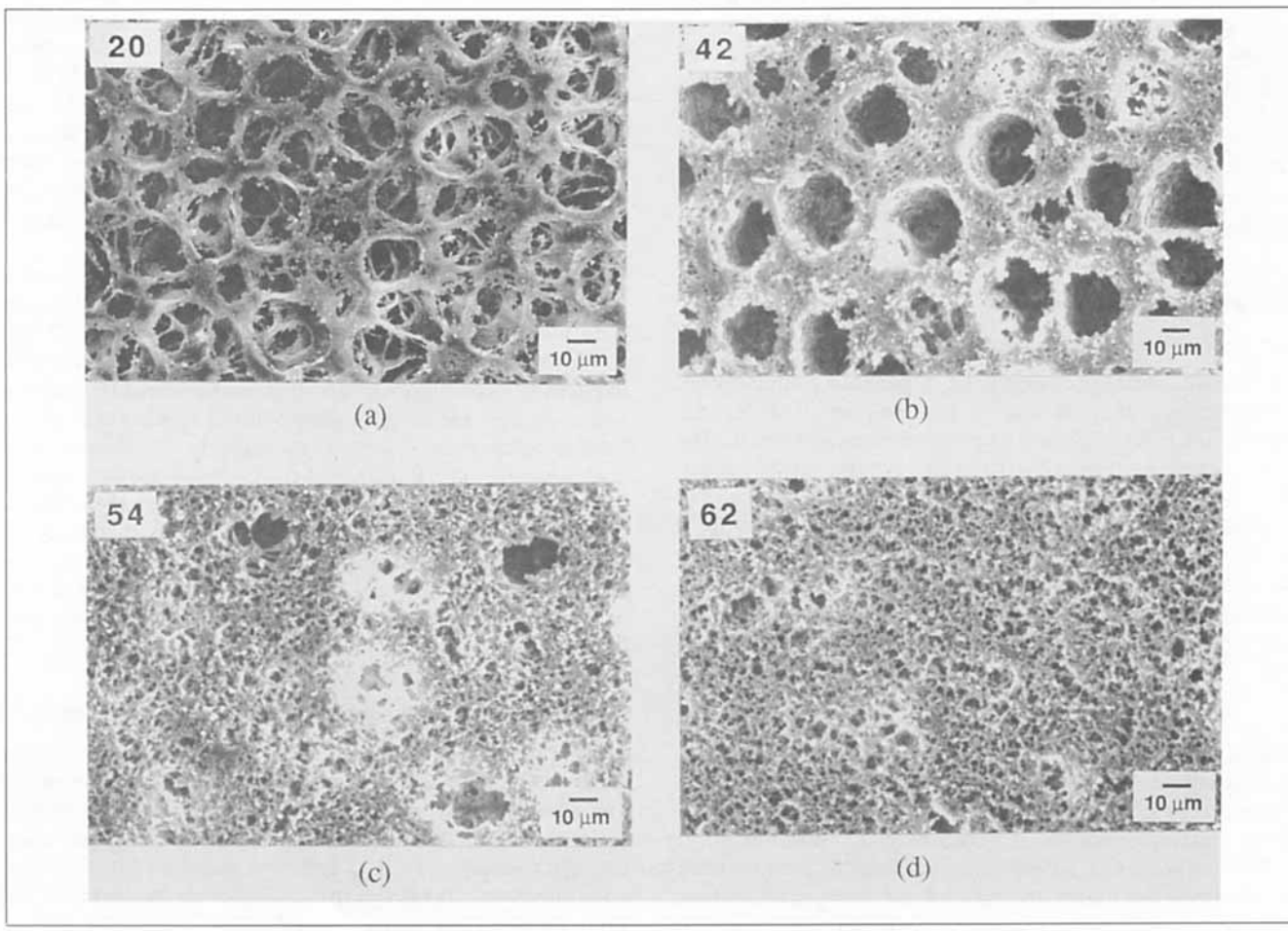

Figure 1. SEM micrographs of the bottom surfaces of alumina-cellulose acetate composites containing (a) 20, (b) 42, (c) 54 and (d) 62 vol. % alumina.

composites. At lower alumina contents, the pore structure consists of large pores (15-μm-diameter) which are oriented through the thickness of the film. As the alumina content is increased, the large pores disappear leading eventually to a more uniform smaller pore network (1–2μm-diameter). At all ceramic contents, the pores are interconnected. The free standing films ranged in thickness from approximately 30 to 100 μm with increasing alumina content and, in all cases, had top surfaces that were rich in polymer. The asymmetry of these composite structures was shown in a previous publication (Wara et al., 1995). The distribution of the alumina particles in the cellulose acetate matrix is demonstrated in Figure 2. Secondary and backscattered images of a 42 vol. % alumina composite clearly show that the alumina particles (brighter in backscattered mode) have remained unagglomerated and are uniformly distributed within the interconnected cellulose acetate phase.

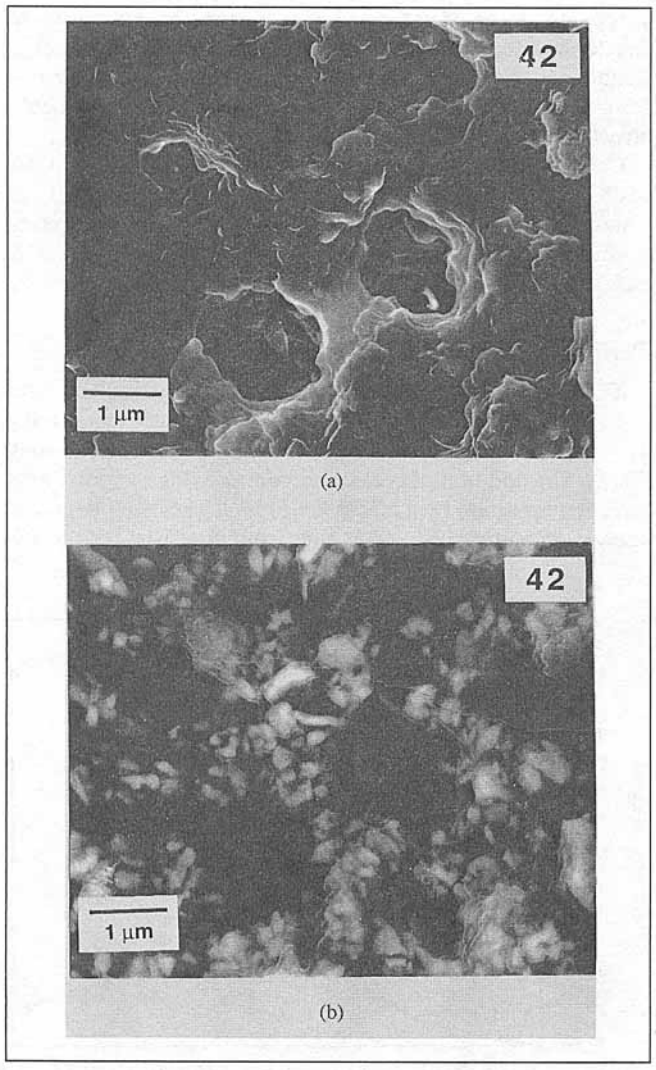

Figure 2. (a) Secondary and (b) backscattered SEM micrographs at high magnification of an alumina-cellulose acetate composite containing 42 vol. % alumina.

Accelerating voltage was 10 kV.

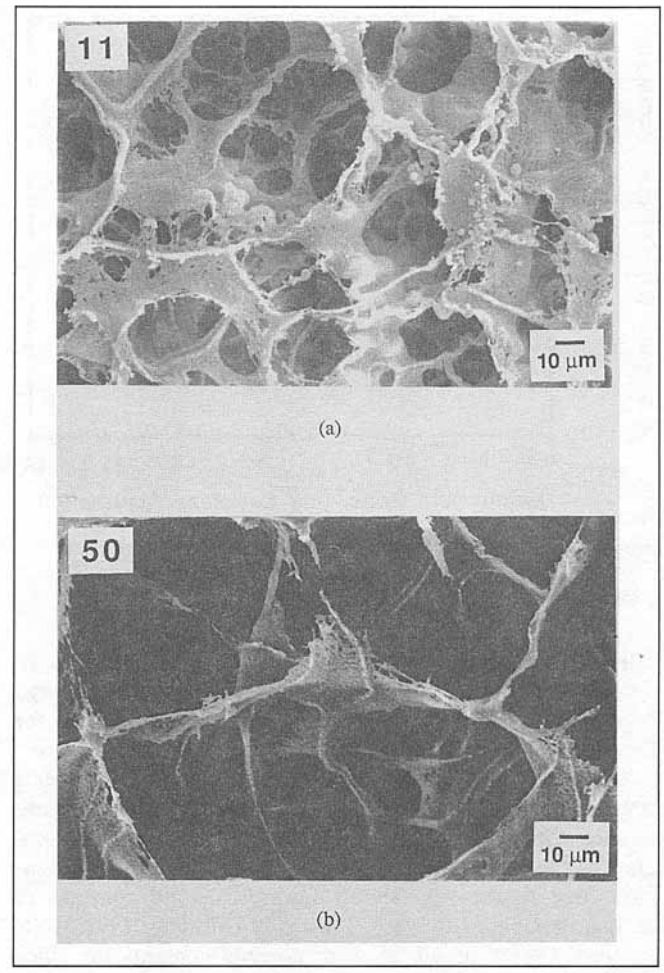

Figure 3. SEM micrographs of the bottom surfaces of silica-cellulose acetate composites containing (a) 11 and (b) 50 vol. % silica.

The microstructure of composites containing base-stabilized silica did not vary with ceramic content. Over a broad range of silica contents, large pores remain the dominate microstructural feature in the silica-cellulose acetate composites (Figure 3). Furthermore, backscattered electron investigations suggest that the silica is agglomerated and not incorporated into the polymer matrix.

Dispersion characterization

The adsorption isotherm for cellulose acetate on the surface of acid-stabilized alumina is given in Figure 4. Cellulose acetate adsorbs on the alumina particle surfaces up to about 3.7 mg/m^2 of alumina. Initially, the rise in polymer adsorption is rapid. In this region, all of the polymer adsorbs on the particle surfaces leaving no free polymer in the dispersion. Dispersions from this region of the graph (0–20-mg cellulose acetate/mL) form composites with higher relative vol. % alumina; these composites had a smaller pore microstructure (Figures 1c and 1d). As the particle surfaces become saturated with polymer, however, the adsorption levels out and excess polymer remains in the suspension. Composites prepared from dispersions in this region of the graph (> 20-mg

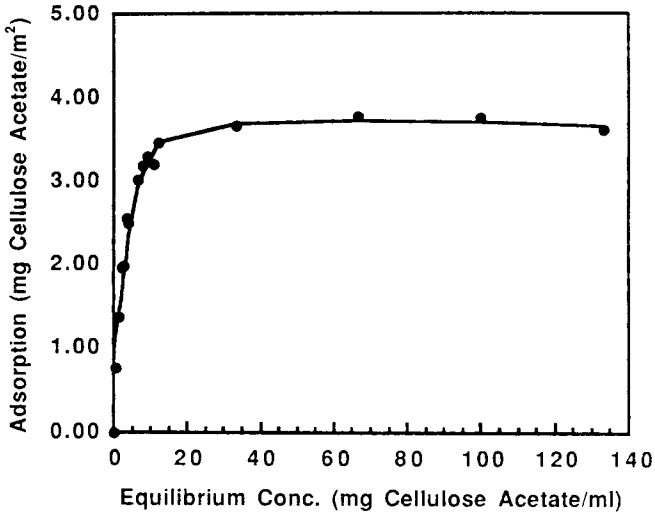

Figure 4. Adsorption isotherm for cellulose acetate on the surface of acid-stabilized alumina.

cellulose acetate/mL) had lower amounts of alumina compared with polymer, and their microstructures contained large pores. No adsorption of cellulose acetate was observed for the base-stabilized silica particles.

The effect of solvent composition on alumina and silica stability is shown in Figure 5a. In the absence of cellulose acetate, the alumina particles become unstable and agglomerate as the acetone content is increased. The particles destabilize due to the significantly lower dielectric constant of acetone compared to water [21 vs. 79 (Moreno, 1992a)]. By contrast, over a broad range of acetone contents the silica particles remain stable. The circle denotes the experimental solvent condition used to make the composite coatings. At this composition, the alumina is completely agglomerated while the silica is still relatively stable. Figure 5b shows the effect of cellulose acetate addition on particle stability at the experimental solvent composition. As the cellulose acetate content increases, the alumina particles become more stable. Data points from approximately 4 to 8 g cellulose acetate correspond to the cellulose acetate/alumina ratios used for composite processing. The addition of cellulose acetate appears to destabilize the silica. Since cellulose acetate does not adsorb on the silica surface, this destabilization is attributed to depletion flocculation effects caused by the free (unadsorbed) polymer.

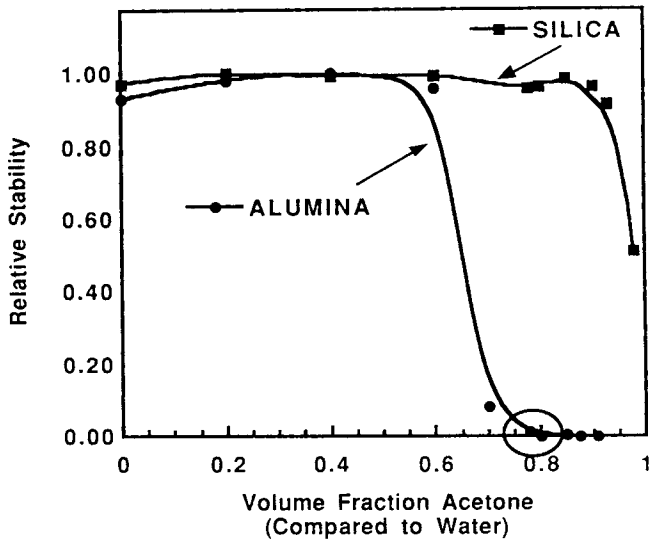

Figure 5a. Relative stability vs. acetone content for acid-stabilized alumina and base-stabilized silica.

Circle indicates the 3.6 to 1 ratio of acetone to water used for composite processing.

Composite firing and ceramic microstructure

Fired macroporous ceramic films were prepared from alumina-cellulose acetate composites. Ceramic films could be made from all composites with greater than 40 vol. % alumina. Examples of composites and subsequent fired ceramics are presented in Figure 6. The SEM images suggest that the pore sizes (both the large 15 μm pores and the smaller 1–2 μm pores) do not significantly change from the composites to the fired ceramics and the interconnectivity of the pores is maintained. Furthermore, upon firing, the dense polymer-rich layer at the top surface collapsed resulting in more symmetric structures.

Composites made from dispersions containing base-stabilized silica and cellulose acetate did not yield coherent ceramic films. During firing, the silica-cellulose acetate composites fall apart as the polymer is removed. After firing, only isolated clumps of silica remain.

Particle consolidation studies

TGA data for a 42 vol. % alumina-cellulose acetate film are shown in Figure 7. Cellulose acetate begins decomposing at ~ 260°C and is completely eliminated by approximately 500°C. The addition of greater amounts of alumina only shifts the decomposition by a maximum of 5°C. The TGA data also show a secondary burnout region from approximately 330°C

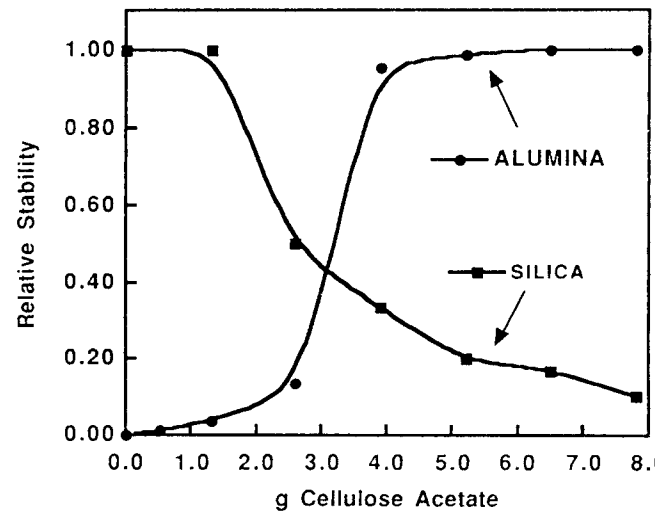

Figure 5b. Effect of cellulose acetate content on relative stability of acid-stabilized alumina and base-stabilized silica.

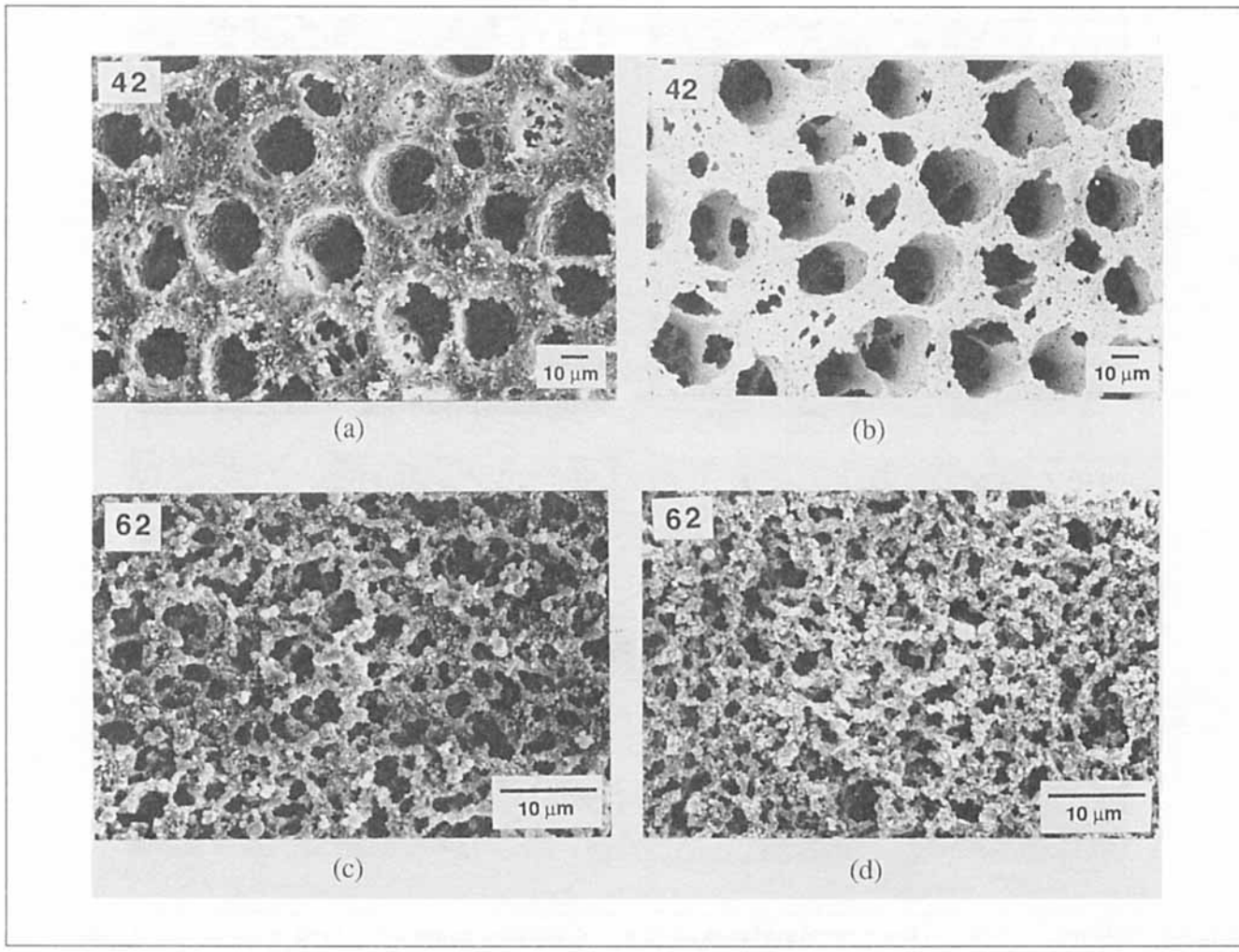

Figure 6. SEM micrographs of the bottom surfaces of: (a) 42 vol. % alumina composite; (b) corresponding fired ceramic; (c) 62 vol. % alumina composite; (d) corresponding fired ceramic.

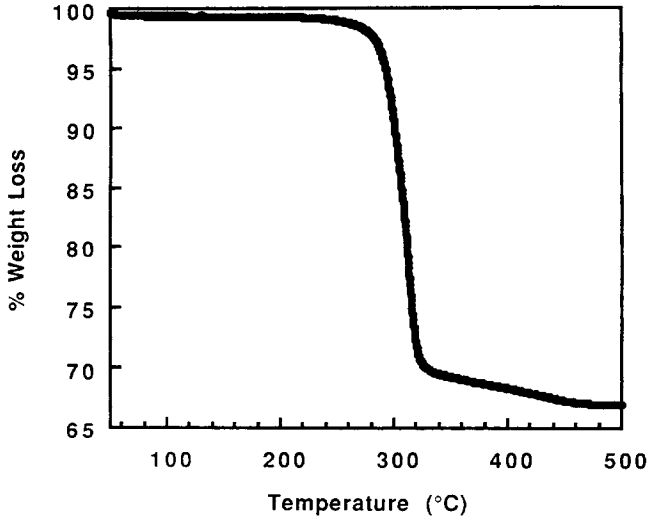

Figure 7. Thermogravimetric analysis of an alumina-cellulose acetate composite containing 42 vol. % alumina.

Heating rate was 1°C/min.

to 500°C. Based on visual observations, this region corresponds to oxidation of residual carbon. DTA results confirm these burnout observations. Furthermore, DMA shows a glass transition with associated softening of cellulose acetate at approximately 190°C.

To understand particle consolidation during firing, composites were heated to different stages in the burnout and then observed by SEM. Based on the TGA data (Figure 7), the areas of interest are: (i) before polymer burnout (< 260°C); (ii) the initial stages of polymer removal (260–300°C); (iii) an intermediate burnout temperature (300–330°C); (iv) the later stages of polymer removal (330–500°C). SEM images from these regions are given in Figure 8. Before burnout begins, the alumina particles are imbedded in the polymer matrix (Figure 8a). As polymer starts to burn out, the bulk spaces between the particles hollow out due to polymer removal and the particle shapes become more defined (Figure 8b). By 310°C, distinct particles can be distinguished with thin discontinuous polymer layers on their surfaces. The distances between particles also decrease (Figure 8c). Finally, the polymer is no longer visible, and particle-particle contacts can be discerned (Figure 8d).

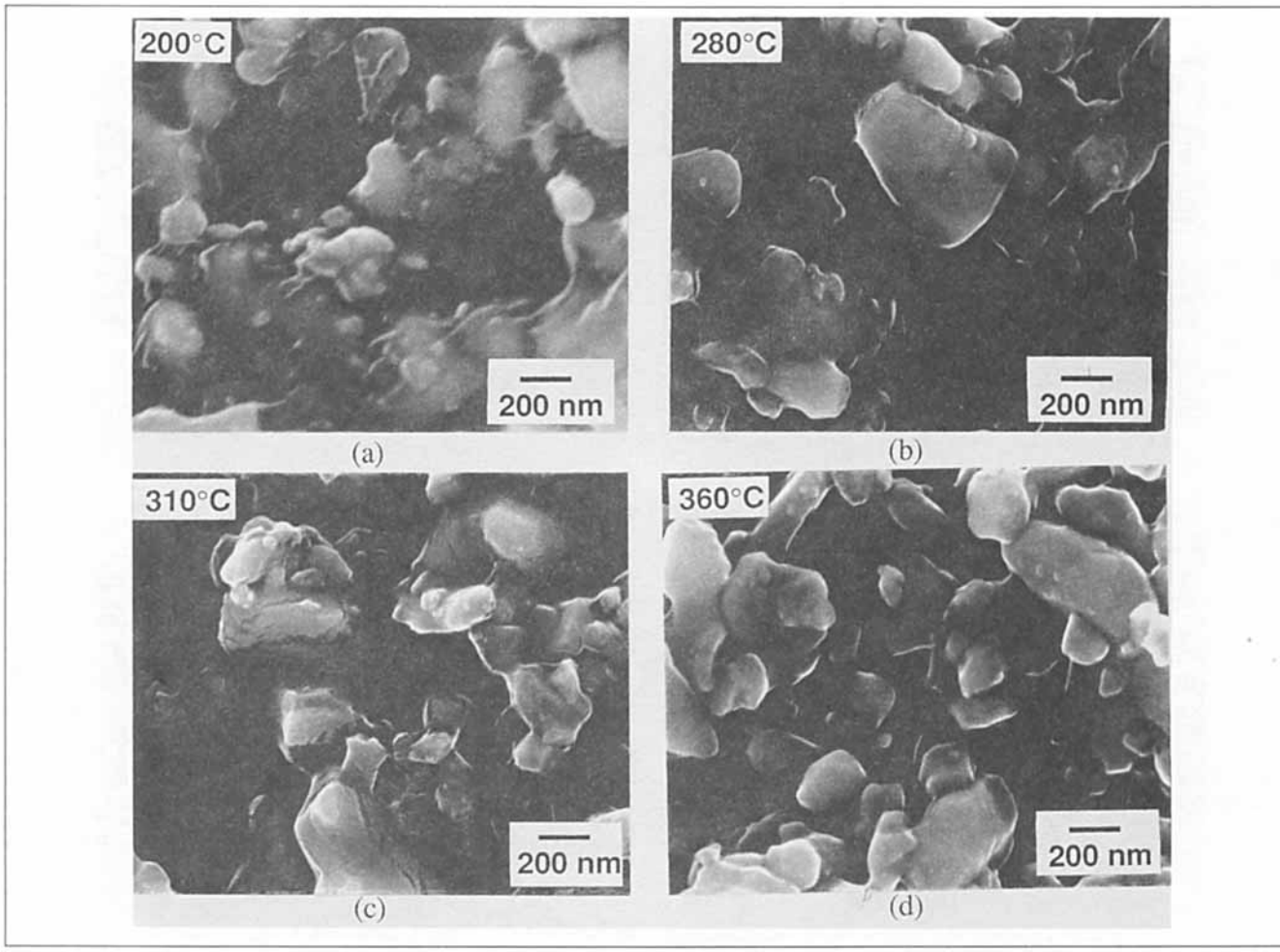

Figure 8. SEM micrographs of the bottom surfaces of 42 vol. % alumina composites fired to (a) 200°C, (b) 280°C, (c) 310°C and (d) 360°C.

The volume shrinkage due to firing depends on the relative vol. % alumina in the composites, as shown in Figure 9. With increasing alumina content, the overall shrinkage decreases.

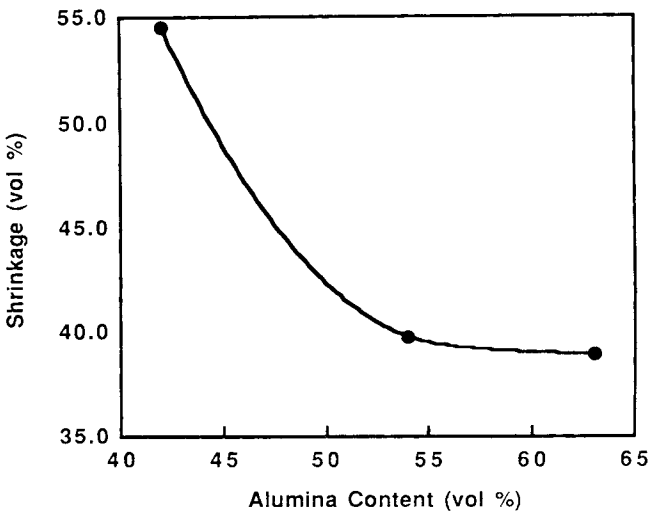

Figure 9. Effect of alumina content on shrinkage of the composites on firing.

However, even at higher alumina contents (62 vol. % Al_2O_3), the overall shrinkage of the composites is still approximately 40 vol. %. Mercury porosimetry results for a 63 vol. % composite and subsequent fired ceramic are shown in Figure 10. During firing, the number of 1 μm pores is significantly reduced, but the larger pore diameters are only slightly decreased. This trend is observed for all alumina composites that yielded coherent ceramic films. Figure 11 shows a 62 vol. % alumina composite and a subsequent fired ceramic. Despite significant shrinkage during firing, the final ceramic sheet retains the shape of the original composite and is crack-free. The free-standing ceramic films could be easily handled and, although the mechanical properties were not measured, the structural integrity increased with increasing ceramic content. Furthermore, since the initial alumina particles are completely crystalline, the fired alumina film is also completely crystalline.

Discussion

Dispersions and composite microstructures

Ceramic-polymer composites were prepared using polymeric phase inversion techniques. The phase separation and, hence, composite microstructures were influenced by the type

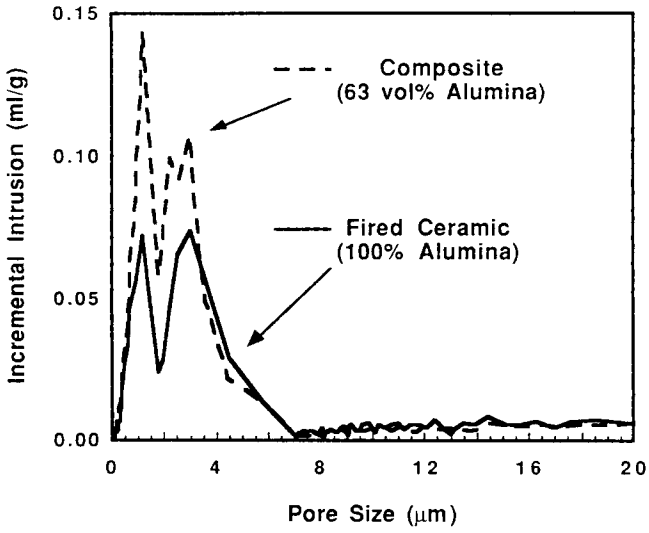

Figure 10. Incremental intrusion volume of mercury as a function of pore diameter for a 63 vol. % alumina composite and a corresponding fired ceramic.

and relative amount of ceramic added to the cellulose acetate solution. With alumina, the composite microstructure was a function of ceramic content, and the ceramic particles were well dispersed in the cellulose acetate matrix. By contrast, composites made with silica contained particle agglomerates and little variation in composite microstructure was possible. The ability to change the pore structure with increasing ceramic content in the alumina composites provides a simple method for microstructural control. Furthermore, a uniform distribution of ceramic particles is crucial to achieving coherent macroporous ceramics after firing.

To understand the effect of the ceramic on the composite microstructure, the interaction between the ceramic and polymer in the dispersion must first be examined. The adsorption study shows that cellulose acetate adsorbs on alumina surfaces but not on silica. This behavior is a consequence of the ceramic surface characteristics; alumina at pH 4 has a basic surface according to the Lewis terminology

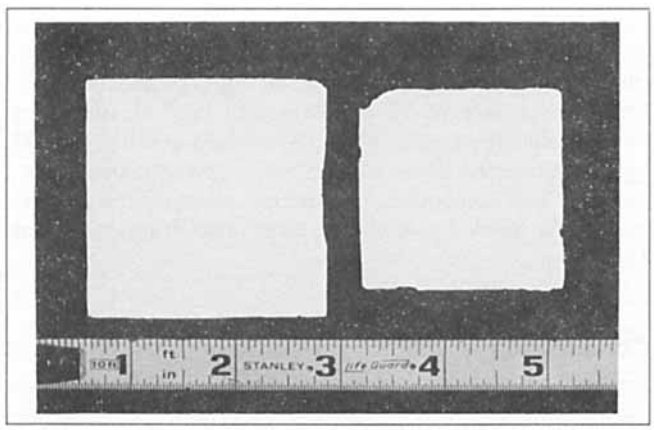

Figure 11. Alumina composite, 62 vol. % (left), and the corresponding fired ceramic (right).

(Jensen, 1980), while silica stabilized at pH 9 has an acidic surface. The hydroxyl on cellulose acetate preferentially associates with the basic surface of alumina. The adsorption of cellulose acetate on alumina is necessary to stabilize the alumina particles. As shown in Figure 5a, electrostatic mechanisms (stabilization with HCl) alone are not sufficient to stabilize the alumina particles in the low dielectric constant acetone/water solution (the solvent conditions used for composite processing). Cellulose acetate adsorption, however, provides steric stabilization (Figure 5b). This stabilization of alumina by cellulose acetate is expected based on comparison with other polymers which are known to sterically stabilize alumina (such as poly(vinyl butyral), poly(vinyl acetate), poly(methacrylic acid) (Moreno, 1992b; Cesarano et al., 1988; Howard et al., 1990; Pugh, 1994)). At equivalent molecular weights, these polymers typically exhibit adsorptions of the same magnitude as those shown in Figure 4 (in the range of 1–5 mg/m^2) (Cesarano et al., 1988; Howard et al., 1990; Pugh, 1994). The unagglomerated state of the alumina particles in the composites is a direct result of the steric stabilization caused by cellulose acetate adsorption.

Interactions between the polymer and the ceramic surfaces are responsible for the unagglomerated alumina particles, but ceramic-polymer interactions do not account for the agglomeration of the silica particles in the composites or the final ceramic distributions. These characteristics can be explained by more closely examining the polymeric phase inversion process. This examination will also suggest reasons why pore structure is a direct function of ceramic concentration in the casting dispersions.

Phase inversion, as mentioned in the introduction, is a phase separation process induced through nonsolvent immersion. For the cellulose acetate/acetone/water system, acetone is the solvent for the polymer and water is the nonsolvent. Under conditions used in this study, the compositions of the casting dispersions lie in the one-phase region of the ternary phase diagram (Strathmann et al., 1971; Shojaie et al., 1994) and are, thus, homogeneous. Upon immersion in a water bath, the coating is driven into the two-phase region of the phase diagram. Phase separation begins at the surface and proceeds downward through the coating thickness (Tsay and McHugh, 1990; Kesting and Fritzsche, 1993). Pore formation in these systems is dictated by the phase separation process. Upon entering the two-phase region, the coating segregates by interdiffusion of the components into polymer rich/acetone and polymer lean/water domains (Kesting and Fritzsche, 1993). A number of theories have been presented on the mechanism of this separation and, specifically, why larger pores (referred to as macrovoids) form (Smolders et al., 1992; Paulsen et al., 1994). Recently, Limbert (1996) used cryo-SEM studies to show that smaller pore formation is the result of nucleation and growth of the polymer-lean phase. The polymer-rich phase forms the matrix, and after removal of volatiles the polymer-lean regions become pores. If the polymer-rich phase has not vitrified due to solvent loss after nucleation and growth of the polymer-lean phase (Li et al., 1996; Koros and Pinneau, 1994), the polymer-rich regions will rupture due to continued solvent/nonsolvent exchange and the smaller polymer-lean regions will coalesce. The larger polymer-lean regions which result from this process become macrovoids upon drying (Limbert, 1996). The larger pores

observed in the ceramic-polymer films resemble these macrovoids and may form by a similar mechanism.

Based on the dispersion characterization and the mechanisms of phase inversion, the ceramic distribution in the composites can be explained. For alumina, the cellulose acetate adsorbs on the particle surfaces. Consequently, during phase separation, the alumina particles are forced to associate with the polymer rich phase. Upon completion of phase separation, the alumina particles which are predominately coated with adsorbed polymer become trapped in the polymer matrix. Furthermore, since the alumina was initially unagglomerated and well dispersed, the particles remain unagglomerated and uniformly distributed within the polymer (Figure 2). In the case of silica, no polymer adsorption occurs. Consequently, the silica does not segregate to the polymer-rich regions of the phase-separated dispersion and is not trapped in the matrix. As the composites dry after deposition, the silica particles continue to agglomerate as the dispersion medium evaporates. The result is an agglomerated silica phase which is not incorporated into the polymer.

Polymer adsorption may also explain why the pore structure shifts from larger pores to more uniform small pores as the ceramic content is increased. Initial cryo-SEM studies on alumina-cellulose acetate materials suggest that large pores form as the polymer-rich matrix, which surrounds smaller polymer-lean pockets, is ruptured. The incorporation of a ceramic phase into the polymer matrix (the result of polymer adsorption) may stiffen the matrix and suppress rupture. Consequently, as more ceramic is added, large pores are suppressed. This work will be the subject of a future article.

Conversion to porous ceramics

The ceramic distribution is a crucial factor for successful composite firing. Alumina-cellulose acetate composites with their uniformly distributed ceramic phase yield macroporous ceramics while silica-cellulose acetate systems do not. The amount of ceramic in the composites is also important. Only composites with a relative alumina content greater than approximately 40 vol. % rendered coherent ceramic films. These factors suggest that to successfully fire a composite the ceramic particles must not only be distributed uniformly, but they also have an upper limit on separation distance. This link between particle configuration (both distribution and separation distance) and successful firing leads to a central issue: how is the polymer removed and the original composite shape retained, or, stated more fundamentally, what is the mechanism of particle-particle consolidation during the firing process?

TGA results show that cellulose acetate should burn out of the composites by ~ 500°C. For alumina, the ceramic particles do not begin to sinter until approximately 900°C, leaving a 400°C gap. (While such a gap is commonplace in processing of dense ceramics from powders (Parish et al., 1990; Sun et al., 1988; Shih et al., 1988; Cima and Lewis, 1988; Barone et al., 1988), the tenuous nature of porous composite structures makes polymer removal and the establishment of particle-particle contacts a critical issue in these systems.) SEM results clearly show that the alumina films maintain the microstructures of the original composites (Figure 6). Consequently, the ceramic particles must come together before the polymer completely burns out of the films. Based on this conclusion, the mechanism for ceramic consolidation can be deduced by tracking composite microstructure during polymer burnout.

The mechanism for alumina particle consolidation is shown through the SEM photos taken at different stages of the firing process (Figure 8). This study reveals that particle-particle contact is established as polymer is removed from the particle surfaces and, specifically, from the regions of closest contact between the particles. As the polymer goes through its glass transition (~ 190°C), its viscosity decreases. This change may allow capillary forces to draw the particles closer together until contact. Since this contact is established far below the sintering temperature of alumina, van der Waals interactions and gravitational effects keep the ceramic structure together until sintering begins. These effects are very similar to the consolidating forces present during the tape casting or injection molding of dense ceramics after the polymers used in these processes have been removed (Moreno, 1992b; Dow et al., 1988; Bohnlein-Maub et al., 1992).

The proposed mechanism for particle consolidation explains how the alumina particle network is established from the composites to the ceramic films. However, this mechanism does not explain why the structures shrink a minimum of 40 vol. % without a significant change in pore diameters. The mercury porosimetry results shed light on this discrepancy. During firing, pores with diameters of 1 μm or less are eliminated. These pores are on the order of the particle diameters and are probably squeezed out, in part, as the alumina particles are drawn together. Further removal of small pores is also possible due to solid state sintering at high temperatures. Consequently, shrinkage results mainly from the elimination of submicron pores and the particles coming together as the polymer is removed.

The flexibility of the processing method for making macroporous ceramics is shown in this discussion. The ceramic firing study shows that macroporous ceramics can be made from phase inversion composites if two criteria are met: (1) the ceramic is well distributed in the polymer matrix; and (2) a minimum ceramic loading is attained. In turn, these two criteria can be achieved when an interaction exists between the ceramic surfaces and the polymer chains. Based on these observations, tailored macroporous ceramics can be made using this method by manipulating the ceramic-polymer interactions in combined dispersions. For example, cellulose acetate-silica systems were examined using silica with a basic surface (Ludox Cl, the silica has an alumina surface layer). The basic surface of the silica (as with pure alumina) promoted cellulose acetate adsorption which resulted in uniformly distributed silica particles within the cellulose acetate matrix. These composites, as expected based on the processing criteria, yielded porous silica films upon firing (see Figure 12).

Conclusions

Polymer-based phase inverse techniques offer a new and flexible method for processing macroporous ceramics. Macroporous ceramics with controlled microstructures were fired from ceramic-polymer composites. Successful ceramic

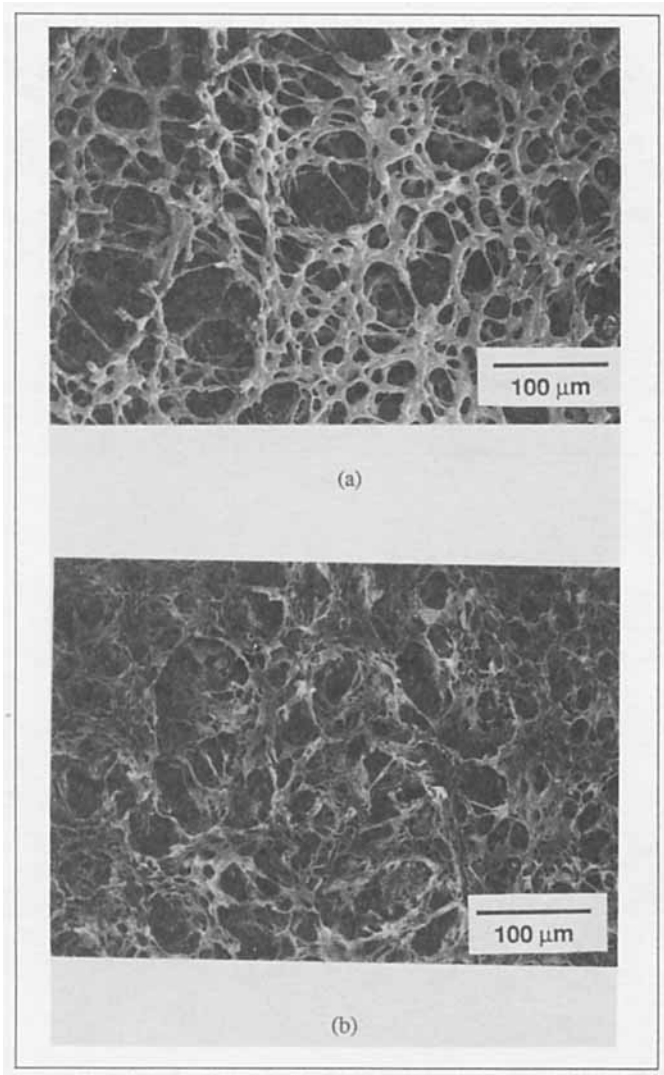

Figure 12. SEM micrographs of the bottom surfaces of (a) 53 vol. % acid-stabilized silica composite and (b) corresponding fired ceramic.

processing required a well distributed ceramic particle phase in the composites and a minimum ceramic loading. These criteria were achieved in systems where the polymer phase adsorbed on the ceramic particle surfaces (alumina). By manipulating the ceramic surface to promote polymer adsorption, tailoring of macroporous ceramics was demonstrated for the case of silica.

Acknowledgments

Support from the 3M Company and the National Science Foundation (DMR-9357502) are gratefully acknowledged. The authors thank Jason A. Payne for assistance with dynamic mechanical analysis experiments. The use of facilities at the Center for Interfacial Engineering Microscopy Center is also acknowledged.

Literature Cited

Barone, M., J. Ulicny, R. Hengst, and J. Pollinger, "Removal of Organic Binders in Ceramic Powder Compacts," *Ceramic Powder Sc. II*, G. L. Messing, E. R. Fuller, and H. Hausner, eds., Ceramic Transactions, **1**, 575 (1988).

Bohnlein-Maub, J., W. Sigmund, G. Wegner, W. H. Meyer, F. Hebel, K. Seitz, and A. Roosen, "The Function of Polymers in the Tape Casting of Alumina," *Adv. Mater.*, **4**, 73 (1992).

Brave, R. R., *Inorganic Membranes: Synthesis, Characterization, and Applications*, Van Nostrand Reinhold, New York (1991).

Cesarano, J., I. A. Aksay, and A. Bleier, "Stability of Aqueous α-Al_2O_3 Suspensions with Poly(methacrylic acid) Polyelectrolyte," *J. Amer. Cer. Soc.*, **71**, 250 (1988).

Cima, M. J., and J. A. Lewis, "Firing-Atmosphere Effects on Char Content from Alumina-Polyvinyl Butyral Films," *Ceramic Powder Science II*, G. L. Messing, E. R. Fuller, and H. Hausner, eds., Ceramic Transactions, **1**, 567 (1988).

Davis, M. E., "Organizing for Better Synthesis," *Nature*, **364**, 391 (1993).

de Lange, R. S. A., J. H. A. Hekkink, K. Keizer, and A. J. Burggraaf, "Permeation and Separation Studies on Microporous Sol-Gel Modified Ceramic Membranes," *Microporous Materials*, **4**, 169 (1995).

Dow, J., M. Sacks, and A. Shenoy, "Dispersion of Ceramic Particles in Polymer Melts," *Ceramic Powder Science II*, G. L. Messing, E. R. Fuller, and H. Hausner, eds., Ceramic Transactions, **1**, 380 (1988).

Howard, K. E., C. D. E. Lakeman, and D. A. Payne, "Surface Chemistry of Various Poly(vinyl butyral) Polymers Adsorbed onto Alumina," *J. Amer. Ceram. Soc.*, **73**, 2543 (1990).

Jensen, W. B., *The Lewis Acid-Base Concepts: An Overview*, Wiley, New York (1980).

Kesting, R. E., and A. K. Fritzsche, *Polymeric Gas Separation Membranes*, Wiley, New York (1993).

Kim, Y. J., "Sol-Gel Processing and Characterization of Macroporous Titania Coatings," PhD Thesis, Univ. of Minnesota, Minneapolis (1995).

Klein, L. C., and N. Giszpenc, "Sol-Gel Processing for Gas Separation Membranes," *Amer. Cer. Soc. Bull.*, **69**, 1821 (1990).

Koros, W. J., and I. Pinneau, "Membrane Formation for Gas Separation Processes," *Polymeric Gas Separation Membranes*, D. R. Paul and Y. P. Yampol'skii, eds., p. 209 (1994).

Li, S. G., T. van den Boomgaard, C. A. Smolders, and H. Strathmann, "Physical Gelation of Amorphous Polymers in a Mixture of Solvent and Nonsolvent," *Macromol.*, **29**, 2053 (1996).

Limbert, A., "Microstructure Development in Coatings by Cryogenic Scanning Electron Microscopy," MS Thesis, Univ. of Minnesota, Minneapolis (1996).

Marquis, P. M., "High Performance Bioceramics," *Chemistry in Britain*, **28**, 245 (1993).

McDonogh, R. M., C. J. D. Fell, and A. G. Fane, "Characteristics of Membranes Formed by Acid Dissolution of Polyamides," *J. Memb. Sci.*, **31**, 321 (1987).

Moreno, R., "The Role of Slip Additives in Tape Casting Technology: I. Solvents and Dispersants," *Amer. Cer. Soc. Bull.*, **71**, 1521 (1992a).

Moreno, R., "The Role of Slip Additives in Tape Casting Technology: II. Binders and Plasticizers," *Amer. Cer. Soc. Bull.*, **71**, 1647 (1992b).

Mulder, M. H. V., J. O. Hendrikman, J. G. Wijmans, and C. A. Smolders, "A Rationale for the Preparation of Asymmetric Pervaporation Membranes," *J. Appl. Poly. Sci.*, **30**, 2805 (1985).

Parish, M. V., J. D. Hodge, and C. R. Hubbard, "Thermal and Phase Analysis of $YBa_2Cu_3O_{7-x}$ Powder Compacts with Organic Acid Additives," *Ceramic Powder Science III*, G. L. Messing, S. Hirano, and H. Hausner, eds., Ceramic Transactions, **12**, 803 (1990).

Paulsen, F. G., S. S. Shojaie, and W. B. Krantz, "Effect of Evaporation Step on Macrovoid Formation in Wet-Cast Polymeric Membranes," *J. Memb. Sci.*, **91**, 265 (1994).

Pugh, R. J., "Dispersion and Stability of Ceramic Powders in Liquids," *Surface and Colloid Chemistry*, Advanced Ceramic Processing, **7**, 127 (1994).

Schaefer, D. W., "Engineered Porous Materials," *MRS Bull.*, **14**, 14 (1994).

Sheppard, L. M., "Porous Ceramics: Processing and Applications," *Porous Materials*, K. Ishizaki, L. M. Sheppard, S. Okada, T. Hamasaki, and B. Huybrechts, eds., Ceramic Transactions, **31**, 3 (1993).

Shih, W. K., G. W. Scheiffele, Y. N. Sun, and J. W. Williams, "Pyrolysis of Poly(vinyl butyral) Binders: I. Degradation Mechanisms,"

Ceramic Powder Science II, G. L. Messing, E. R. Fuller, and H. Hausner, eds., Ceramic Transactions, **1**, 549 (1988).
Shojaie, S. S., W. B. Krantz, and A. R. Greenberg, "Dense Polymer Film and Membrane Formation Via the Dry-Cast Process: II. Model Validation and Morphological Studies," *J. Membrane Sci.*, **94**, 281 (1994).
Smith, W. A., "The Role of Piezocomposites in Ultrasonic Transducers," *Ultrasonic Symp.*, IEEE, 755 (1989).
Smolders, C. A., A. J. Reuvers, R. M. Boom, and I. M. Wienk, "Microstructures in Phase-Inversion Membranes. Part 1. Formation of Macrovoids," *J. Memb. Sci.*, **73**, 259 (1992).
Strathmann, H., P. Scheible, and R. W. Baker, "A Rationale for the Preparation of Leob-Sourirajan-Type Cellulose Acetate Membranes," *J. Appl. Poly. Chemistry*, **15**, 811 (1971).
Sun, Y. N., M. D. Sacks, and J. W. Williams, "Pyrolysis Behavior of Acrylic Polymers and Acrylic Polymer/Ceramic Mixtures," *Ceramic Powder Science II*, G. L. Messing, E. R. Fuller, and H. Hausner, eds., Ceramic Transactions, **1**, 538 (1988).
Tanev, P. T., and T. J. Pinnavaia, "Biomimetic Templeting of Porous Lamellar Silicas by Vesicular Surfactant Assemblies," *Science*, **271**, 1267 (1996).
Tsay, C. S., and A. J. McHugh, "Mass Transfer Modeling of Asymmetric Membrane Formation by Phase Inversion," *J. Poly. Sci.: Part B Poly. Phys.*, **28**, 1327 (1990).
Wara, N. M., B. V. Velamakanni, and L. F. Francis, "Addition of Alumina to Cellulose Acetate Membranes," *J. Memb. Sci.*, **104**, 43 (1995).

Manuscript received Oct. 28, 1996, and revision received Apr. 16, 1997.